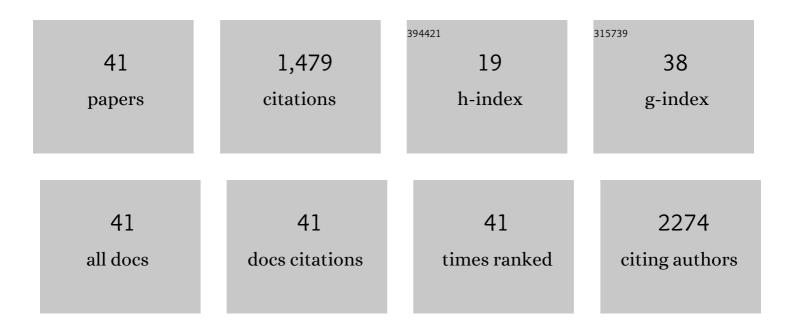
Lan Xiang

List of Publications by Year in descending order

Source: https://exaly.com/author-pdf/453112/publications.pdf Version: 2024-02-01



LAN XIANC

#	Article	IF	CITATIONS
1	Li-rich layered oxides: Structure, capacity and voltage fading mechanisms and solving strategies. Particuology, 2022, 61, 1-10.	3.6	21
2	Graded Preparation and Industrial Applications of Large-Ball Polyolefin Catalyst Carriers. Catalysts, 2022, 12, 117.	3.5	4
3	Synergistic Effect of Mn ³⁺ Formation–Migration and Oxygen Loss on the Near Surface and Bulk Structural Changes in Single Crystalline Lithium-Rich Oxides. ACS Applied Materials & Interfaces, 2021, 13, 3891-3898.	8.0	13
4	Estimation of Reaction Heat in Ti-Bearing Blast Furnace Slag—Sulfuric Acid System Based on Mechanical Mixture Model. Mining, Metallurgy and Exploration, 2021, 38, 1247-1252.	0.8	2
5	Synergetic effect of high Ni ratio and low oxygen defect interface zone of single crystals on the capacity retention of lithium rich layered oxides. Journal of Colloid and Interface Science, 2021, 594, 485-492.	9.4	9
6	Designed synthesis of ZnO/Pd@ZIF-8 hybrid structure for highly sensitive and selective detection of methane in the presence of NO2. Sensors and Actuators B: Chemical, 2021, 344, 130220.	7.8	22
7	Hydrothermal Synthesis of (001) Facet Highly Exposed ZnO Plates: A New Insight into the Effect of Citrate. Crystals, 2019, 9, 552.	2.2	15
8	Reduced Graphene Oxide/Mesoporous ZnO NSs Hybrid Fibers for Flexible, Stretchable, Twisted, and Wearable NO ₂ E-Textile Gas Sensor. ACS Sensors, 2019, 4, 2809-2818.	7.8	114
9	Tuning the Nanoarea Interfacial Properties for the Improved Performance of Li-Rich Polycrystalline Li-Mn-O Spinel. ACS Applied Materials & Interfaces, 2019, 11, 14796-14802.	8.0	17
10	UV light irradiation enhanced gas sensor selectivity of NO2 and SO2 using rGO functionalized with hollow SnO2 nanofibers. Sensors and Actuators B: Chemical, 2019, 290, 443-452.	7.8	112
11	Effects of Cationic Polyacrylamide on Hydrothermal Formation of Ultralong α aSO ₄ ·0.5H ₂ O Whiskers. Crystal Research and Technology, 2019, 54, 1800224.	1.3	4
12	Facile synthesis of mesoporous ZnO sheets assembled by small nanoparticles for enhanced NO2 sensing performance at room temperature. Sensors and Actuators B: Chemical, 2018, 270, 207-215.	7.8	42
13	Hybrid graphene/cadmium-free ZnSe/ZnS quantum dots phototransistors for UV detection. Scientific Reports, 2018, 8, 5107.	3.3	21
14	Near infrared light enhanced room-temperature NO2 gas sensing by hierarchical ZnO nanorods functionalized with PbS quantum dots. Sensors and Actuators B: Chemical, 2018, 255, 2538-2545.	7.8	73
15	Removal of SO42â ^{^,} from Li2CO3 by Recrystallization in Na2CO3 Solution. Crystals, 2018, 8, 19.	2.2	12
16	Sprayed, Scalable, Wearable, and Portable NO ₂ Sensor Array Using Fully Flexible AgNPs-All-Carbon Nanostructures. ACS Applied Materials & Interfaces, 2018, 10, 34485-34493.	8.0	74
17	Preparation of Hierarchical CaSO ₄ Whisker and Its Reinforcing Effect on PVC Composites. Journal of Nanomaterials, 2018, 2018, 1-7.	2.7	9
18	3D Architectured Graphene/Metal Oxide Hybrids for Gas Sensors: A Review. Sensors, 2018, 18, 1456.	3.8	83

Lan Xiang

#	Article	IF	CITATIONS
19	Efficient and Reversible Electron Doping of Semiconductor-Enriched Single-Walled Carbon Nanotubes by Using Decamethylcobaltocene. Scientific Reports, 2017, 7, 6751.	3.3	36
20	Understanding Mn-Based Intercalation Cathodes from Thermodynamics and Kinetics. Crystals, 2017, 7, 221.	2.2	13
21	A Review on the Fabrication of Hierarchical ZnO Nanostructures for Photocatalysis Application. Crystals, 2016, 6, 148.	2.2	91
22	Confined Formation of Ultrathin ZnO Nanorods/Reduced Graphene Oxide Mesoporous Nanocomposites for High-Performance Room-Temperature NO ₂ Sensors. ACS Applied Materials & Interfaces, 2016, 8, 35454-35463.	8.0	210
23	Ligand-directed rapid formation of ultralong ZnO nanowires by oriented attachment for UV photodetectors. Journal of Materials Chemistry C, 2016, 4, 5755-5765.	5.5	23
24	Hierarchical ZnO Nanosheet-Nanorod Architectures for Fabrication of Poly(3-hexylthiophene)/ZnO Hybrid NO ₂ Sensor. ACS Applied Materials & Interfaces, 2016, 8, 8600-8607.	8.0	106
25	Influence of NH ₄ Cl on Hydrothermal Formation of <i>α</i> -CaSO ₄ ·0.5H ₂ O Whiskers. Journal of Nanomaterials, 2015, 2015, 1-6.	2.7	4
26	Ultra-rapid formation of ZnO hierarchical structures from dilution-induced supersaturated solutions. CrystEngComm, 2014, 16, 7115-7123.	2.6	36
27	Effect of Mg ²⁺ on Hydrothermal Formation of α-CaSO ₄ ·0.5H ₂ O Whiskers with High Aspect Ratios. Langmuir, 2014, 30, 9804-9810.	3.5	75
28	Influence of Sodium Dodecyl Sulfonate on the Formation of ZnO Nanorods from <i>ε</i> -Zn(OH) ₂ . Journal of Nanomaterials, 2013, 2013, 1-6.	2.7	2
29	Influence of the Mixing Ways of Reactants on ZnO Morphology. Journal of Nanomaterials, 2013, 2013, 1-6.	2.7	3
30	Synthesis of Al(OH)3Nanostructures from Al(OH)3Microagglomerates via Dissolution-Precipitation Route. Journal of Nanomaterials, 2013, 2013, 1-6.	2.7	5
31	Synthesis and Surface Characterization ofγ-MnO2Nanostructures. Journal of Nanomaterials, 2013, 2013, 1-6.	2.7	8
32	Low-Dimensional Inorganic Nanofunctional Materials: Design, Assembly, and Application for Chemical Engineering (I). Journal of Nanomaterials, 2013, 2013, 1-2.	2.7	0
33	PROGRESS IN THE HYDROTHERMAL FORMATION OF DISPERSIVE NANO-PARTICLES AND WHISKERS. , 2012, , .		0
34	Green co-precipitation byproduct-assisted thermal conversion route to submicron Mg ₂ B ₂ O ₅ whiskers. CrystEngComm, 2011, 13, 1654-1663.	2.6	25
35	Repair the Pores and Preserve the Morphology: Formation of High Crystallinity 1D Nanostructures via the Thermal Conversion Route. Crystal Growth and Design, 2011, 11, 709-718.	3.0	11
36	Influence of sodium dodecyl sulfate on the fabrication of zinc oxide nanoparticles. Research on Chemical Intermediates, 2011, 37, 281-289.	2.7	3

Lan Xiang

#	Article	IF	CITATIONS
37	Formation of calcium sulfate whiskers from CaCO3-bearing desulfurization gypsum. Research on Chemical Intermediates, 2011, 37, 449-455.	2.7	47
38	Synthesization and crystallization mechanism of nano-scale γ-AlOOH with various morphologies. International Journal of Minerals, Metallurgy and Materials, 2010, 17, 376-379.	4.9	9
39	Successive effect of rolling up, oriented attachment and Ostwald ripening on the hydrothermal formation of szaibelyite MgBO2(OH) nanowhiskers. CrystEngComm, 2009, 11, 1910.	2.6	36
40	Different nanostructures of boehmite fabricated by hydrothermal process: effects of pH and anions. CrystEngComm, 2009, 11, 1338.	2.6	79
41	Simulation of the adsorption of CaCl2 on Mg(OH)2 planes. Journal of Materials Science, 2008, 43, 2387-2392.	3.7	10